SCIENCE CHINA
Life Sciences

•COVER ARTICLE•

March 2018 Vol.61 No.3: 253–265
https://doi.org/10.1007/s11427-017-9222-9

TRPC3 is required for the survival, pluripotency and neural differentiation of mouse embryonic stem cells (mESCs)

Helen Baixia Hao[1], Sarah E. Webb[1], Jianbo Yue[2], Marc Moreau[3], Catherine Leclerc[3] & Andrew L. Miller[1*]

[1]*Division of Life Science and State Key Laboratory of Molecular Neuroscience, HKUST, Clear Water Bay, Hong Kong, China;*
[2]*Department of Biomedical Sciences, City University of Hong Kong, Hong Kong, China;*
[3]*Centre de Biologie du Développement (CBD), Centre de Biologie Intégrative (CBI), Université de Toulouse, CNRS, UPS, Toulouse F-31062, France*

Received August 10, 2017; accepted November 6, 2017; published online January 31, 2018

Transient receptor potential canonical subfamily member 3 (TRPC3) is known to be important for neural development and the formation of neuronal networks. Here, we investigated the role of TRPC3 in undifferentiated mouse embryonic stem cells (mESCs) and during the differentiation of mESCs into neurons. CRISPR/Cas9-mediated knockout (KO) of *TRPC3* induced apoptosis and the disruption of mitochondrial membrane potential both in undifferentiated mESCs and in those undergoing neural differentiation. In addition, *TRPC3* KO impaired the pluripotency of mESCs. *TRPC3* KO also dramatically repressed the neural differentiation of mESCs by inhibiting the expression of markers for neural progenitors, neurons, astrocytes and oligodendrocytes. Taken together, our new data demonstrate an important function of TRPC3 with regards to the survival, pluripotency and neural differentiation of mESCs.

transient receptor potential canonical subfamily member 3 (TRPC3), mouse embryonic stem cells (mESCs), neuron differentiation, CRISPR/Cas9, pluripotency, apoptosis, mitochondrial membrane potential

Citation: Hao, H.B., Webb, S.E., Yue, J., Moreau, M., Leclerc, C., and Miller, A.L. (2018). TRPC3 is required for the survival, pluripotency and neural differentiation of mouse embryonic stem cells (mESCs). Sci China Life Sci 61, 253–265. https://doi.org/10.1007/s11427-017-9222-9

INTRODUCTION

Embryonic stem cells (ESCs) have two distinguishing properties, they can proliferate in an unlimited manner (i.e., have the ability to self-renew) and they can differentiate into any type of somatic cell (i.e. they are pluripotent) (Bradley et al., 1984; Beddington and Robertson, 1989). It is because of these properties that ESCs have the potential for use in cell-based therapies to treat a range of congenital, developmental, and degenerative conditions, including neurodegenerative diseases (McNeish, 2004; Hipp and Atala, 2008). Thus, elucidating the cellular and molecular mechanisms that regulate neural fate determination from stem cells is a crucial first step before they can be successfully applied to regenerative medicine (Liu et al., 2013; Engel et al., 2016).

The neural differentiation of ESCs is a dynamic and complex process, which is regulated by combinatorial signaling pathways, and involves intrinsic transcription factors, cytokines, and growth factors, as well as epigenetic modifications (Dhara and Stice, 2008; Hayashi et al., 2008; Chuang et al., 2015). In addition, Ca^{2+} is a versatile and universal intra- and inter-cellular second messenger, which is known to be vital for embryonic neurogenesis (Berridge et al., 2003; Leclerc et al., 2012). Ca^{2+} signaling is also reported to be key for regulating the differentiation of ESCs into neuronal progenitor cells. For example, antagonizing the

*Corresponding author (email: almiller@ust.hk)

activity of RyR2 (an ER-located Ca^{2+} release channel), CD38 (an enzyme that catalyzes the synthesis of cADPR and NAADP), neuronatin (a SERCA2 inhibitor), or STIM1 (an ER Ca^{2+} sensor), resulted in an inhibition of the neural differentiation of mouse ESCs (mESCs) (Yu et al., 2008; Lin et al., 2010; Hao et al., 2014; Wei et al., 2015; Hao et al., 2016). The role of several of the transient receptor potential canonical (TRPC) channels in neural differentiation has also been investigated. For example, the inhibition of TRPC channel members 1 and 4 (TRPC1, TRPC4; both Ca^{2+} influx channels), has been shown to impair the proliferation of neuroepithelial cells and block neurite extension in post-mitotic neurons derived from human ESCs (hESCs) (Weick et al., 2009). The contribution, however, of many other Ca^{2+} channels or pumps to the regulation of neural differentiation of ESCs is still largely unknown. However, numerous studies have shown that TRPC member 3 (TRPC3) is abundantly expressed in the brain, and various attributed functions in the central nervous system (CNS) have been described (Fusco et al., 2004; Amaral and Pozzo-Miller, 2007). For example, using a *TRPC3* knockout (KO) mouse model, it was proposed that *TRPC3* mediates mGluR-dependent synaptic transmission in cerebellar Purkinje cells, and is crucial for motor coordination (Hartmann et al., 2008).

TRPC3 is a nonselective cation channel, which is permeable to both Na^{+} and Ca^{2+} (Lichtenegger and Groschner, 2014). It is proposed to contribute to downstream Ca^{2+} signal transduction via the integration of multiple signals resulting from receptor-induced phospholipase C (PLC) activation (Trebak et al., 2003; Vazquez et al., 2003; Kwan et al., 2006; Soboloff et al., 2007). TRPC3 activity has also been linked to a variety of neural processes, as well as several neuropathophysiological conditions. For example in the dominant *Moonwalker* (*Mwk*) mouse mutant, a gain-of-function mutation (T635A) in *TRPC3* has been shown to result in abnormal channel gating, which led to cerebellar ataxia (Becker et al., 2009; Becker, 2014; Hanson et al., 2015). A similar situation has been observed in humans, where a mutation in *TRPC3* (R762H) was reported to result in adult-onset cerebellar ataxia (Fogel et al., 2015). Another study demonstrated that Ca^{2+} signaling is activated to a greater extent in the *Mwk* mutant than in the wild-type mouse, and this results in a disruption of lipid homeostasis, as well as impaired dendritic growth and synapse formation during Purkinje cell development in the cerebellum (Dulneva et al., 2015). In various other studies, TRPC3 has also been reported to promote cell survival, control dendritic remodeling, and mediate growth cone guidance by regulating Ca^{2+} transients in different types of neurons (Li et al., 2005; Amaral and Pozzo-Miller, 2007; Jia et al., 2007; Louhivuori et al., 2015).

Thus, although some functions of TRPC3 have been identified, its role in regulating the pluripotency and neural differentiation of mESCs is still poorly understood. By genetically knocking-out (KO) the expression of *TRPC3* in mESCs via CRISPR/Cas9, we investigated the role of this channel in regulating the viability, pluripotency, and neural differentiation of these cells. Here, we report that the expression of *TRPC3* mRNA and TRPC3 protein increases as mESCs undergo neural differentiation. In addition, following *TRPC3*-KO via CRISPR/Cas9 gene editing, apoptosis was induced, and the normal mitochondrial membrane potential was disrupted in both undifferentiated mESCs and in cells undergoing neural differentiation. Furthermore, *TRPC3* KO also impaired the pluripotency and neural differentiation of mESCs.

RESULTS

The expression of TRPC3 gradually increased during the neural differentiation of mESCs

Sox1-GFP 46C mESCs were cultured in ESGRO medium without a fibroblast feeder layer. They then spontaneously differentiated into cells of the neural lineage via adherent monolayer culture with N2B27 medium. The identity of neural progenitor cells could be monitored during differentiation via the expression of Sox1-GFP (Ying et al., 2003; Ying and Smith, 2003). Indeed, as Figure 1A–C shows, the expression of Sox1-GFP was first observed at day 4 of neural differentiation when 27.6%±4.25% of the population expressed the marker. The number of Sox1-GFP cells reached a maximum of 56.90%±3.37% at day 6 of neural differentiation, after which there was a slow decrease as the cells differentiated into specific neuronal and glial cell types (Figure 1C). Immunolabeling was also used to demonstrate the presence of pluripotent cells at day 0 (via the expression of Oct4 and SSEA1), and neural progenitor cells at day 6 (via the expression of Sox1 and Nestin), as well as glia and neurons at day 10 (via the expression of Tuj1 and GFAP, respectively; Figure 1D).

We have previously reported the dynamic expression of various Ca^{2+} signaling proteins during the neural differentiation of mESCs (Zhang et al., 2013; Hao et al., 2014; Wei et al., 2015). Here, we examined the expression pattern of *TRPC3* mRNA and TRPC3 protein during this process using qRT-PCR, Western blot and immunocytochemistry (Figure 2). The expression of *TRPC3* mRNA in undifferentiated mESCs (i.e., on day 0) was relatively weak but then it increased from day 4 to day 10 (Figure 2A(a)). Similarly, the expression of TRPC3 protein increased in neural progenitor cells at day 4 and day 6, when compared with the undifferentiated cells, and exhibited a further increase in differentiated neurons (see day 10) (Figure 2A(b) and B).

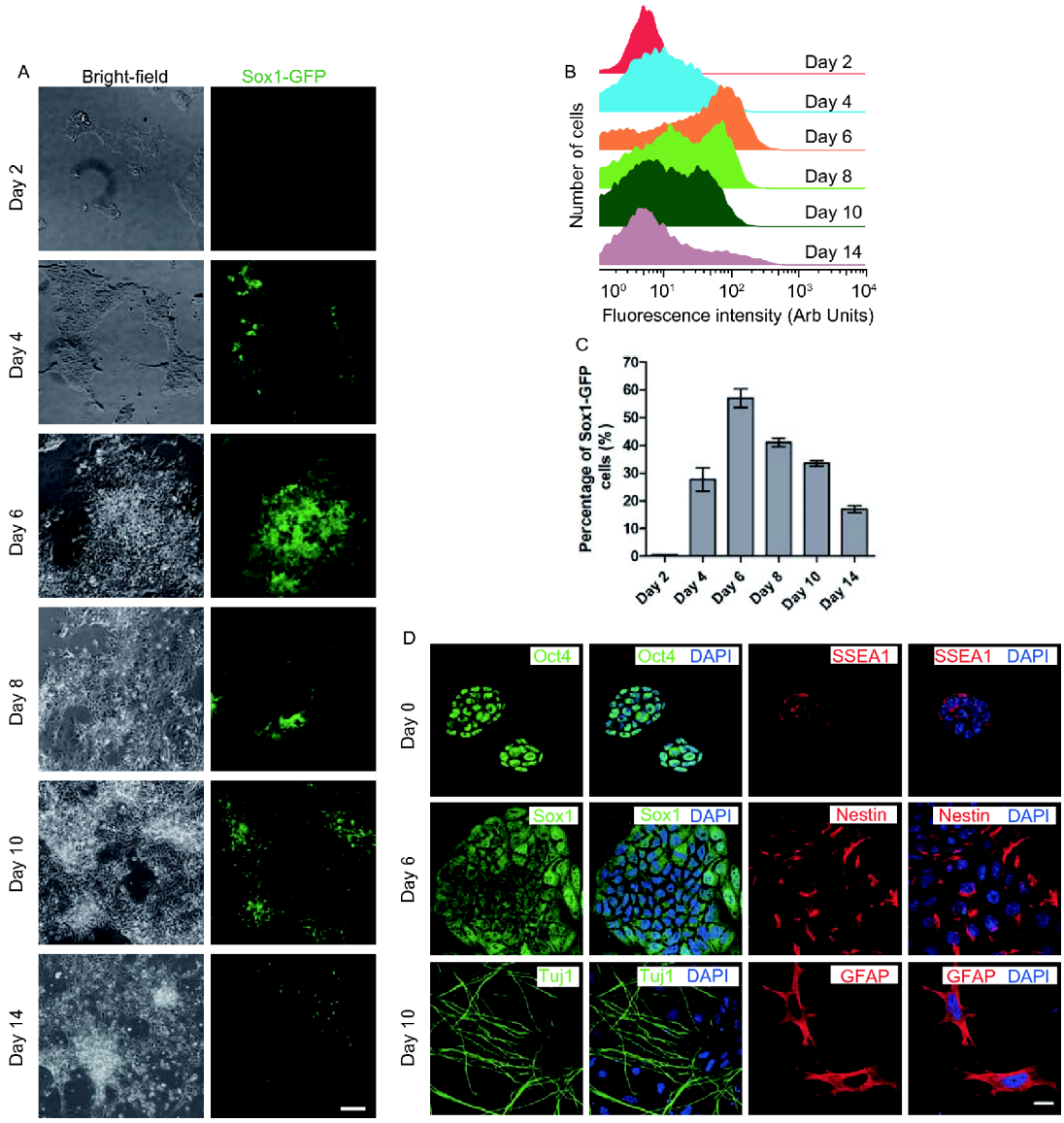

Figure 1 The neural differentiation of Sox1-GFP 46C mESCs by an *in vitro* monoculture method. A, Bright-field and Sox1-GFP fluorescence images of mESCs at Day 2 to Day 14 of neural differentiation. B, Flow cytometry analysis showing the dynamic expression of Sox1-GFP during neural differentiation of mESCs at the times indicated. C, Quantification of the Sox1-GFP expressing cells shown in panel (B). D, Confocal images showing the expression of pluripotency markers (Oct4, SSEA1) on Day 0, neural differentiation markers on Day 6 (Sox1, Nestin), and neuron (Tuj1) and glia (GFAP) markers on Day 10 of differentiation. The nuclei were labeled with DAPI (blue). Scale bars, 100 μm (A) and 20 μm (D). Data are presented as the mean±SE of n=4 experiments.

Generating *TRPC3* KO mESCs

We adapted the CRISPR/Cas9 system to knock out *TRPC3* in mESCs. Thus, two sgRNAs (sgRNA1 and 2), designed to target sequences at exons 2 and 4 of the *TRPC3* gene to introduce insertions/deletions (indels) after a double-stranded break, were generated by Cas9 (Figure 2C). In order to obtain pure mutant clones, single mESC-derived colonies were collected for the identification of *TRPC3* indels. High-resolution melt analysis (HRMA) was used to detect the difference in melting temperature of the homo- and hetero-duplexes containing indels in the mutants, as well as from the non-mutated homo-duplexes in WT and Scr control cells. Five mutant clones were generated for sgRNA1, and five for sgRNA2. For the sgRNA1 mutants, clone 1.1 exhibited a left-shifted peak, when compared with the WT and Scr HRMA curves, whereas clones 1.4, 1.6, 1.7 and 1.9 showed double peaks (Figure 2D). In addition, for the sgRNA2 mutants, clone 2.10 showed a left-shifted HRMA peak, when compared to WT and Scr, whereas clones 2.5, 2.9, 2.11 and 2.12 showed obvious double peaks (Figure 2E). These results indicate that clones 1.1 and 2.10 might be homozygous mutants, whereas the other clones might be heterozygous mutants. To confirm the indels, each clone was sequenced and the sequences were aligned with the WT and Scr sequences (Figure 2F and G). In sgRNA1, clone 1.1 was shown

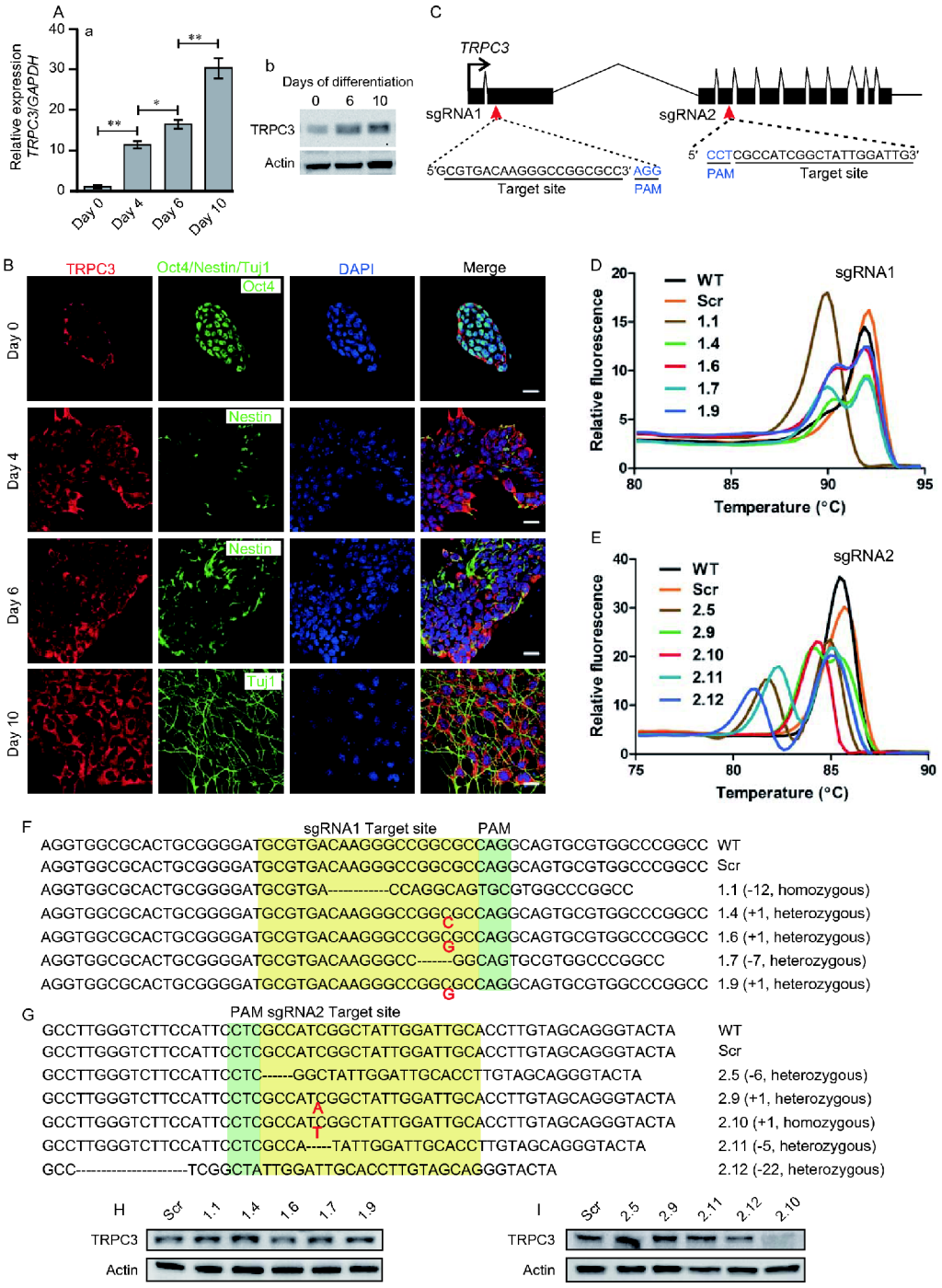

Figure 2 Expression of TRPC3 during neural differentiation of mESCs, and CRISPR/Cas9 knockout of *TRPC3* in undifferentiated mESCs. A(a), qRT-PCR analysis of the relative expression of *TRPC3*, normalized to *GAPDH*, at 0 to 10 days of neural differentiation. Data are presented as the mean±SE of n=3 experiments, and the asterisks indicate statistically significant differences at *, P<0.05 and **, P<0.01. A(b), Western blot to show the expression of TRPC3 at 0, 6 and 10 days of neural differentiation. B, Representative confocal images showing the expression of TRPC3, and either Oct4 (a marker of pluripotency), Nestin (a neural differentiation marker) or Tuj1 (a neuronal marker) in mESCs at 0 to 10 days of neural differentiation. The nuclei were labeled with DAPI (blue). Scale bars, 20 μm. C, Schematic of the *TRPC3* gene showing the two sgRNA target sites. The exons, translational start site and the two sgRNA target sites are shown as black rectangles, a black arrow and two red arrows, respectively. The 20 nucleotide target sequence and NGG protospacer adjacent motif (PAM) are also shown. D and E, High resolution melting analysis graphs to show the melting temperature of the PCR products from the: sgRNA1 (D) and sgRNA2 (E) mutants. F and G, Sequencing of the induced mutations in sgRNA1 (F) and sgRNA2 (G). Deleted bases are marked with dashes, whereas inserted bases are indicated in red at the insertion site. The sgRNA target sites and PAM sequences are highlighted in yellow and green, respectively. H and I, Western blots showing the expression of TRPC3 and actin (internal control) in the: sgRNA1 (H) and sgRNA2 (I) mutants. Wild type (WT) and scrambled (Scr) are wild-type and scrambled sgRNA infected cells, respectively. 1.1–1.9 and 2.5–2.12 indicate the numbers of the different single-cell-derived colonies from the sgRNA1- and sgRNA2-infected mESCs, respectively.

to contain the same mutation (i.e., a 12 nucleotide (nt)-deletion) in both alleles, whereas clones 1.4, 1.6 and 1.9 contained a 1 nt insertion in just one allele, and clone 1.7 contained a 7 nt deletion in just one allele whereas the other allele in these 4 clones had no mutation (Figure 2F). In sgRNA2, clone 2.10 was shown to contain the same mutation (i.e., a 1 nt insertion) in both alleles, whereas the other four clones displayed mutations in one allele only (Figure 2G). In clone 1.1, the 12 nt deletion led to a short-length TRPC3 lacking four amino acids (aa) at sites 78–81, whereas in clone 2.10, the 1 nt insertion resulted in the truncation of the N-terminal 435 aa of TRPC3 due to a shift of the coding frame. In contrast, all the other mutants still produced full-length TRPC3. We showed by Western blot analysis (Figure 2H and I), that the expression of TRPC3 was inhibited in clone 2.10 but there was little difference in the expression of TRPC3 in clone 1.1 or in the other clones when compared with the Scr control. For this reason, clone 2.10 was used for the subsequent experiments.

TRPC3 KO impaired the pluripotency of mESCs

It has been reported that Ca^{2+}-mediated signaling plays a role in the maintenance of pluripotency and cell proliferation of ESCs (Tonelli et al., 2012). Thus, the pluripotency of the *TRPC3* KO and Scr mESCs was compared (Figure 3). Via qRT-PCR, we showed that the level of *Oct4* (a pluripotency marker) (Nichols et al., 1998) was significantly decreased (by ~20%) in the *TRPC3* KO mESCs, when compared with that in the Scr cells (Figure 3A). In addition, when *TRPC3* KO and Scr colonies were stained with alkaline phosphatase (AP; another established marker of pluripotency) (Štefková et al., 2015), all the colonies were labeled to a certain extent although in the case of the *TRPC3* KO cell colonies, some appeared to show a reduced level of AP labeling. What was most obvious, however, was that a proportion of the *TRPC3* KO colonies (24 out of 80 colonies) showed an irregular colony morphology such that the edges were disrupted and the cells were loosely packed. In contrast, the Scr colonies largely (i.e., 79 out of 80 colonies) exhibited tightly packed cells and a well-defined border (Figure 3B). It has been reported that one indication that the pluripotent nature of stem cells is disrupted is an irregular morphology of the cell colony (Nagasaka et al., 2017). Thus, together these results suggest that the pluripotency of mESCs was compromised in the *TRPC3* KO cells.

TRPC3 KO induced apoptosis and the disruption of mitochondrial membrane potential in undifferentiated mESCs and in those undergoing neural differentiation

As maintaining a normal $[Ca^{2+}]_i$ homeostasis is essential for cell survival (Orrenius et al., 2015), the viability of *TRPC3* KO and Scr control mESCs was compared (Figure 4). Using the MTT assay (to determine the metabolic activity of cells), *TRPC3* KO mESCs were shown to exhibit reduced growth when compared with the Scr cells over the 4-day period of culture (Figure 4A). In addition, a higher number of *TRPC3* KO mESCs appeared to be undergoing apoptosis when compared with the Scr controls. This was shown by staining the cells with propidium iodide (PI). Apoptotic cells stain less intensely with PI as the genomic DNA is cleaved into small fragments and there is a consequent reduction in the amount of nuclear DNA (Riccardi and Nicoletti, 2006). With flow cytometry, cells with less intense PI staining exhibit a peak below the G_1 peak (termed the sub-G_1 peak). Our results showed that the ratio of cells in sub-G_1 was significantly higher in the *TRPC3* KO mESCs than in the Scr controls (Figure 4B and C). TUNEL staining was also applied to detect the fragmentation of DNA in both undifferentiated mESCs (at day 0) and during the neural differentiation of mESCs (at days 4-10; Figure 4D and F). In undifferentiated mESCs, there were ~5% more apoptotic cells in the *TRPC3* KO than in the Scr controls. This value increased to 23.4% and 23.7% more at days 4 and 6, respectively, in the *TRPC3* KO cells than in the Scr cells. During later neural differentiation into neurons and glial cells (i.e., day 10), there were still ~10% more apoptotic cells in the *TRPC3* KO cells than in the Scr cells (Figure 4D and F). Together, these results suggest that in the *TRPC3* KO population, there was more apoptosis in both the undifferentiated and neural differentiating cells.

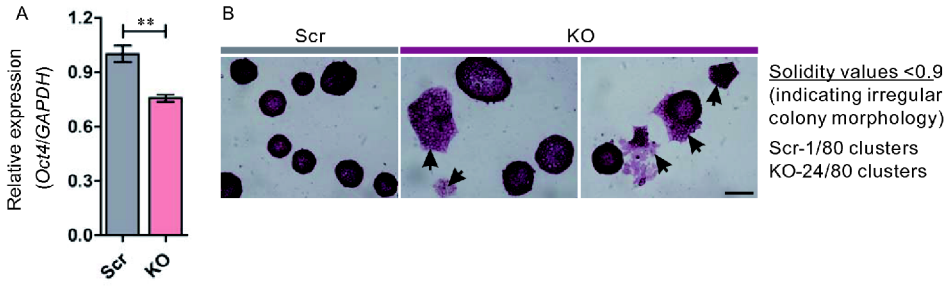

Figure 3 *TRPC3* KO impairs the level of pluripotency of mESCs. A, qRT-PCR analysis of *Oct4* in Scr and *TRPC3* KO mESCs. B, Alkaline phosphatase staining of the Scr and *TRPC3* KO mESCs cultured for 4 days. Black arrows indicate colonies with irregular morphology. Scale bar, 100 μm.

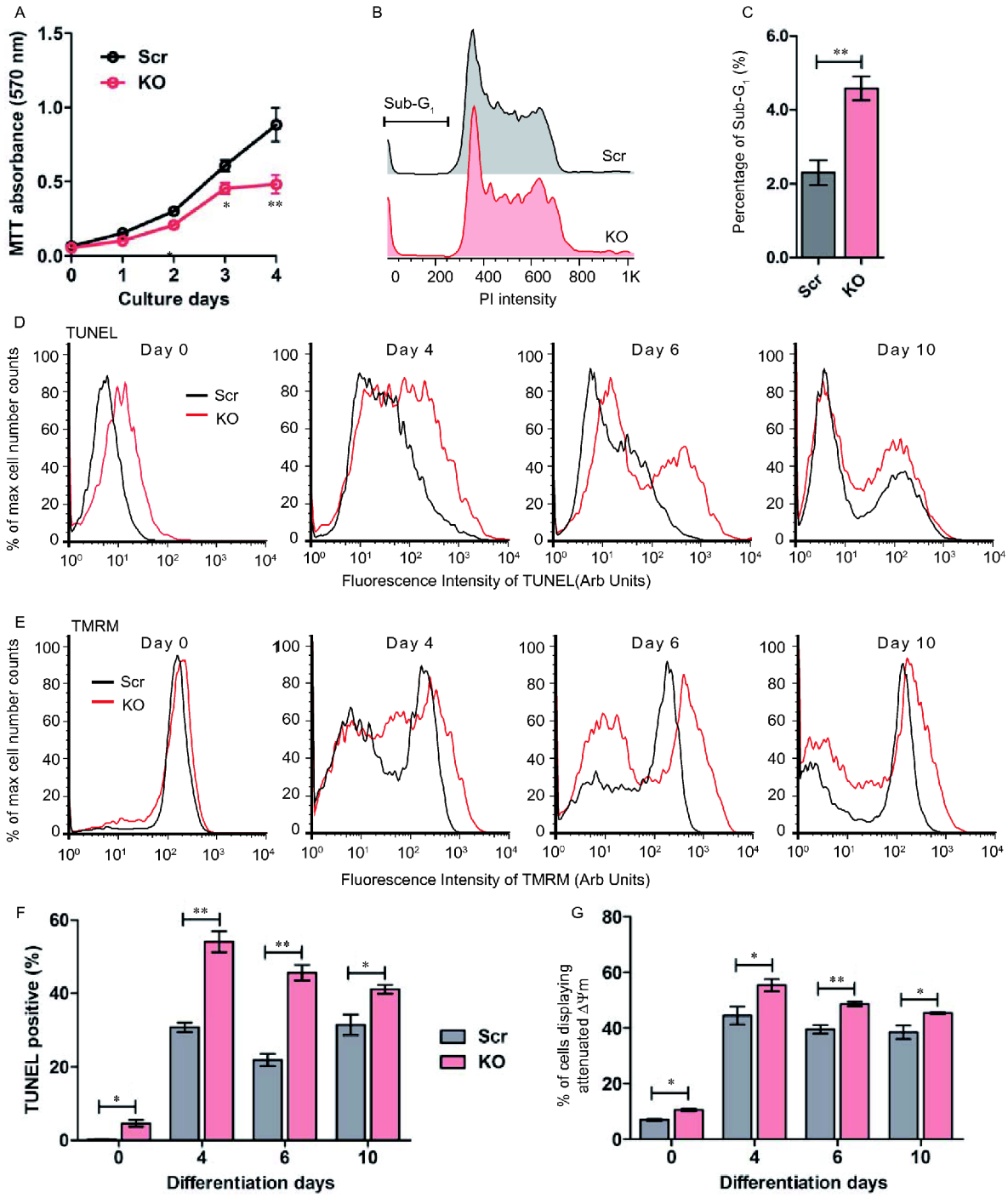

Figure 4 *TRPC3* KO induces apoptosis and the disruption of the mitochondrial membrane potential in undifferentiated mESCs and during neural differentiation of mESCs. A, MTT assay showing the decreased growth curve of *TRPC3* KO mESCs compared with scrambled sequence (Scr) infected mESCs after 4 days in culture. B, Flow cytometry analysis of DNA content following PI staining showing the increased number of *TRPC3* KO mESCs in Sub-G_1 phase when compared with the Scr control. C, Quantification of the percentage of cells in Sub-G_1 phase as shown in the representative example in panel (B). D and E, Flow cytometry analysis following TUNEL (D) and TMRM (E) staining in undifferentiated Scr and *TRPC3* KO mESCs (day 0) and in these cells undergoing neural differentiation at the indicated times (i.e., day 4, 6, and 10), to show the distribution of apoptotic cells and the mitochondrial membrane potential, respectively. F and G, Quantification of the percentage of TUNEL positive (F) and TMRM negative cells (G) in panels (D) and (E), respectively. Data are presented as the mean±SE of n=3 experiments, and the asterisks indicate statistically significant differences at P<0.05 (*) and P<0.01 (**).

As mitochondrial dysfunction is an early indicator of apoptosis, we examined the mitochondrial membrane potential in undifferentiated *TRPC3* KO mESCs and in those undergoing neural differentiation (Figure 4E and G). The use of fluorescent dyes such as TMRM, for measuring the mitochondrial membrane potential are now commonly used to

determine the health or level of injury of cells (Perry et al., 2011). We labeled undifferentiated (day 0) and differentiating (days 4-10) *TRPC3* KO and Scr cells with TMRM and quantified the percent of cells that were TMRM-negative, indicating compromised mitochondrial membranes. Our data showed that in the undifferentiated cells, ~7% and ~10% cells in the Scr and *TRPC3* KO groups, respectively exhibited an attenuated mitochondrial membrane potential. At day 4 of neural differentiation, the percent of TMRM-negative cells in the Scr group increased to ~44.5%, and at days 6 and 10, the percent of cells with an attenuated mitochondrial membrane potential remained relatively high, with values of at ~39.6% and ~38.5%, respectively in this group. In the *TRPC3* KO group, the percent of TMRM-negative cells increased to ~55.4% (at day 4), and remained relatively high with values of ~48.6% and ~45.4% at day 6 and day 10, respectively (Figure 4E and G). In the undifferentiated cells and during neural differentiation, the percent of cells with an attenuated mitochondrial membrane potential was significantly higher in the *TRPC3* KO group than in the Scr group (Figure 4G).

Together, these data suggest that more of the *TRPC3* KO cells were undergoing apoptosis than the Scr cells. This suggests that *TRPC3* might be required for the survival of both undifferentiated mESCs and those undergoing neural differentiation.

TRPC3 KO suppressed the differentiation of neural progenitors, neurons, astrocytes, and oligodendrocytes

As Ca^{2+} signaling has also been reported to play a role in the neural differentiation of mESCs (Zhang et al., 2013; Hao et al., 2014; Wei et al., 2015), the ability of *TRPC3* KO mESCs and Scr control cells to undergo neural differentiation was compared (Figure 5). FACS analysis was conducted to determine the number of Sox1-GFP-expressing cells on day 4 to day 14 (Figure 5A and B). We showed that in the *TRPC3* KO group, there were significantly lower numbers of Sox1-GFP-expressing cells, when compared with those in the Scr group, indicating that the differentiation of neural progenitors might be repressed in these cells. Subsequent qRT-PCR analysis supported the FACS data and showed that in the *TRPC3* KO cells, the expression of *Sox1* and *Nestin* was inhibited at days 4 and 6 of neural differentiation (Figure 5C). qRT-PCR analysis also showed that during the later stages of differentiation (i.e., at days 10 and 14), there was a decreased expression of *Tuj1* and *NeuN* (neuron markers); *TH* and *GFAP* (astrocyte markers); *GAP65* and *Olig1* (oligodendrocyte markers) in the *TRPC3* KO cells compared with the Scr cells (Figure 5C). Taken together, these data suggest that TRPC3 is required for both the early and later stages of neural differentiation, which encompass the specification of mESCs into neural progenitors, followed by differentiation into neurons, astrocytes and oligodendrocytes.

Effect of *TRPC3* KO on the expression of other TRPC isoforms

We applied qRT-PCR to determine the expression level of other *TRPCs* in mESCs with and without *TRPC3* KO. As shown in Figure 6, the expression levels of *TRPC1*, *TRPC2* and *TRPC7* were not affected by *TRPC3* KO. In addition, we were unable to detect the expression of *TRPC4*, *TRPC5* and *TRPC6* in either Scr or *TRPC3* KO mESCs (data not shown). Taken together, these data suggest that *TRPC3* KO did not affect the expression of other *TRPCs* in mESCs.

DISCUSSION

Here, we report the establishment of a stable *TRPC3* KO mESC line using CRISPR/Cas9-based gene editing. *TRPC3* KO resulted in cells with impaired pluripotency that exhibited an increase in apoptosis and a concomitant disruption in the mitochondrial membrane potential. These phenomena were observed in undifferentiated mESCs, as well as in cells undergoing neural differentiation. These data suggest that TRPC3 activity, via the modulation of $[Ca^{2+}]_i$, might be required for the survival, maintenance of pluripotency, and neural differentiation of mESCs. It was clear, however, that the effects of *TRPC3* KO were only partial, suggesting that this channel, although playing an important modulatory role, might not be the only factor regulating these processes. This suggests that other aspects, such as dysfunction of Ca^{2+} and Na^{+} homeostasis, might also contribute to the phenotype and effects we observed.

Ca^{2+} has long been known to play an important role in regulating cell apoptosis by disrupting the function of mitochondria (Orrenius et al., 2015). Persistent and/or excess levels of cytoplasmic Ca^{2+} have been shown to result in the mitochondria being overloaded with Ca^{2+}; this in turn results in a loss of the mitochondrial membrane potential, which leads to apoptosis (Pinton et al., 2008). In addition, TRPC3 is reported to be crucial for regulating Ca^{2+} uptake into the mitochondria and for maintaining the mitochondrial membrane potential (Feng et al., 2013). TRPC3 activity is also reported to be a key factor in the survival of neurons (Jia et al., 2007).

Here, we report that there is an increased amount of apoptosis and a disruption of the mitochondrial membrane potential as Scr mESCs undergo neural differentiation. Such a differentiation-associated apoptosis has been previously described both in neural stem cells (Esdar et al., 2001) and during the neural development of species such as *Caenorhabditis elegans*, *Drosophila melanogaster*, *Danio rerio*,

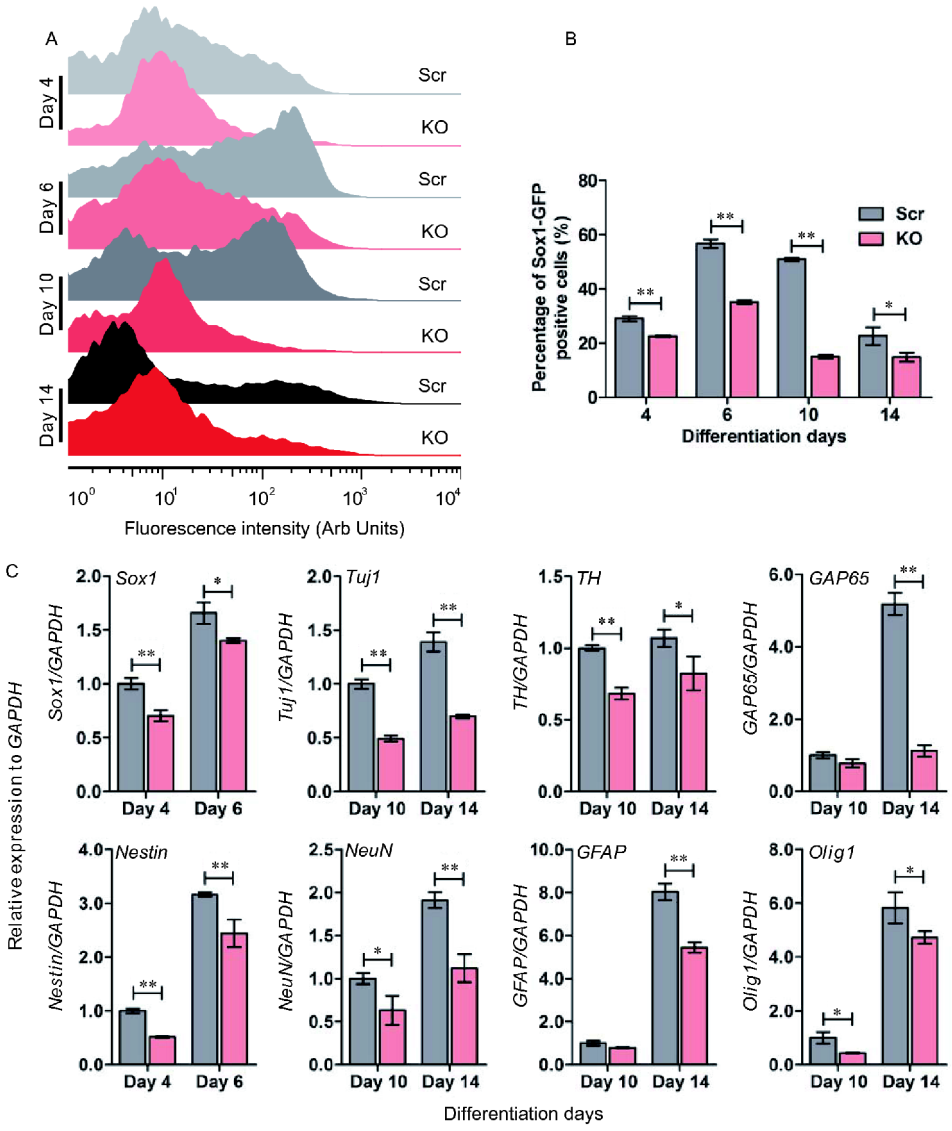

Figure 5 *TRPC3* KO represses the differentiation of mESCs into neural progenitors, neurons, astrocytes and oligodendrocytes. A, Flow cytometry analysis showing the numbers of Sox1-GFP expressing scrambled sequence (Scr) and *TRPC3* KO cells at the indicated times of neural differentiation. B, Quantification of the Sox1-GFP expressing cells shown in panel (A). C, qRT-PCR analysis showing the expression of *Sox1* and *Nestin* (neural progenitor markers); *Tuj1* and *NeuN* (neuron markers); *TH* and *GFAP* (astrocyte markers); and *GAP65* and *Olig1* (oligodendrocyte markers) in Scr and *TRPC3* KO cells at the indicated times of neural differentiation. *GAPDH* was used as the internal control. Data are presented as mean±SE of n=3 experiments and the asterisks indicate statistically significant differences at $P<0.05$ (*) and $P<0.01$ (**).

and *Mus musculus* (reviewed by Yeo and Gautier, 2004). In addition, in the *TRPC3* KO mESCs, apoptosis and a disruption of the mitochondrial membrane potential was induced more in undifferentiated cells and in those undergoing neural differentiation when compared with the Scr control group. We have previously demonstrated that knock down of *Stim1* or over-expression of *Tpc2* or *CD38* induces significant apoptosis during the neural differentiation of mESCs (Zhang et al., 2013; Hao et al., 2014; Wei et al., 2015). Our new results show that when *TRPC3* was knocked out, then apoptosis was induced at least in part by a disruption of the mitochondrial membrane potential in undifferentiated mESCs and in mESCs undergoing neural differentiation. Together with our previous results, this demonstrates the crucial requirement of Ca^{2+} signaling for cell survival during the neural differentiation of mESCs.

TRPC3 KO mESCs also exhibited impaired pluripotency. As disrupting the expression of *Tpc2*, *Stim1*, *Stim2*, *Orai1*, *CD38* or *IP$_3$R3* had little effect on the pluripotency of mESCs (Liang et al., 2010; Zhang et al., 2013; Hao et al., 2014; Wei et al., 2015), our new data suggest that the role of TRPC3 in maintaining pluripotency might be an additional feature of this Ca^{2+} channel. It has previously been reported that mitochondria play a crucial role in the maintenance of pluripotency in both iPSCs and ESCs (Xu et al., 2013). Here, we also report the effect of *TRPC3* KO on the regulation of

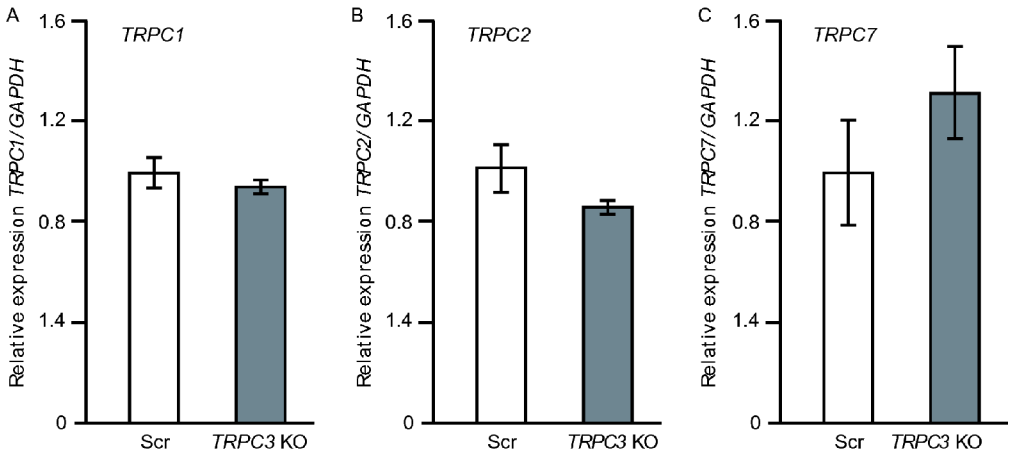

Figure 6 The level of expression of *TRPC1*, *TRPC2* and *TRPC7* was similar in Scr and *TRPC3* KO mESCs. qRT-PCR analysis showing the expression of *TRPC1* (A), *TRPC2* (B) and *TRPC7* (C) in scrambled sequence (Scr) infected mESCs and *TRPC3* KO mESCs. *GAPDH* was used as the internal control. Data are presented as mean±SE of n=3 experiments.

the mitochondrial membrane potential in undifferentiated mESCs. It would be of interest to explore in further detail the link between the function of mitochondria and the maintenance of pluripotency in undifferentiated mESCs by disrupting the function of TRPC3.

We previously reported that several of the Ca^{2+} signaling toolkit proteins, including TPC2, STIM1 and CD38, exhibit a dynamic pattern of expression during the neural differentiation of mESCs, and that they play important roles in regulating neural differentiation (Zhang et al., 2013; Hao et al., 2014; Wei et al., 2015). Here, we report that the expression of TRPC3, another Ca^{2+} signaling toolkit member, was upregulated during the neural differentiation of mESCs, which suggests that it might also play various key roles in regulating neurogenesis. Indeed, we found that in *TRPC3* KO mESCs, the expression of various markers for neural progenitors, neurons, astrocytes, and oligodendrocytes was inhibited (Figure 5), which suggests the requirement of TRPC3 for both early and later neural differentiation. Furthermore, our data are consistent with the robust expression and multiple functions of TRPC3 channels reported in differentiated neurons and glial cells in various *in vitro* and *in vivo* studies (Amaral and Pozzo-Miller, 2007; Hartmann et al., 2008; Louhivuori et al., 2015; Minke and Parnas, 2006).

TRPC3 is recognized to be a nonselective cation channel that is permeable to both Na^+ and Ca^{2+}, and it has been suggested that it might act as a plasma membrane-bound signaling hub (Lichtenegger and Groschner, 2014; Svobodova and Groschner, 2016).The non-selective entry of Na^+ (and Ca^{2+}) into cells via TRPC3 leads to membrane depolarization. Furthermore, the rise in $[Na^+]$ at the cytoplasmic side of the plasma membrane has also been suggested to play a role in Na^+-dependent transport (Eder et al., 2005).

With regards to the effect of *TRPC3* KO on the expression of other TRPC family members, we showed that the expression of *TRPC1*, *2* and *7* was not affected by *TRPC3* KO in mESCs (Figure 6). In addition, *TRPC4*, *5* and *6* were not detected in either the Scr or the *TRPC3* KO mESCs. These data indicate that the defects on the pluripotency, cell survival and mitochondrial membrane potential as well as neural commitment in *TRPC3* KO cells were likely to be a specific effect of *TRPC3* KO.

In summary, we demonstrated that in *TRPC3* KO mESCs, the expression of a number of the key elements in the complex signal transduction networks that are known to initiate and regulate neural induction were perturbed, which might explain why early neural differentiation was impaired. We also identified a number of key processes that result from eliminating TPRC3 activity. These include an increase in apoptosis; and a disruption of the mitochondrial membrane potential. In addition, there is impaired pluripotency; and an inhibition of the expression of markers for neural progenitors, neurons, astrocytes and oligodendrocytes. Taken together, our new data support the proposition of a multifunctional, integrative role for the TRPC3 channel during neural induction, perhaps mediated in part via the regulation of $[Ca^{2+}]_i$, which in a combinatorial manner contributes to the survival, pluripotency, and neural differentiation of mESCs.

MATERIALS AND METHODS

Cell culture

The 46C mESC line, which expressed GFP (knocked-in in the *sox1* locus), was kindly provided by Prof. Austin Smith (Ying et al., 2003). Undifferentiated Sox1-GFP 46C mESCs were maintained in Millipore ESGRO Complete PLUS Clonal Grade medium on 0.1% gelatin-coated plates, and were passaged every 2 days.

HEK 293FT cells (Thermo Fisher Scientific, USA) were maintained in Dulbecco's Modified Eagle Medium (DMEM) with 10% fetal bovine serum (FBS), 6 mmol L^{-1} *L*-glutamine, 1% penicillin-streptomycin (P/S), 1 mmol L^{-1} MEM sodium pyruvate, and 0.1 mmol L^{-1} nonessential amino acids (NEAA).

The neural differentiation of mESCs was induced according to established protocols (Ying et al., 2003; Ying and Smith, 2003), where undifferentiated cells were plated in N2B27 medium on 0.1% gelatin-coated plates and the medium was renewed every 2 days for 2 weeks.

The medium components used for culturing the 293FT cells, and the N2B27 medium used for differentiating the mESCs into neurons were purchased from Thermo Fisher Scientific.

TRPC3 KO with CRISPR/Cas9

The sequences of the sgRNA target sites (i.e., 20 nucleotides (nt) preceding the 5′-NGG PAM sequence) were designed using the online CRISPR Design Tool (http://tools.genome-engineering.org) following the instructions provided in a previous report (Ran et al., 2013). The sequences of the Scr sgRNA, and the two pairs of sgRNA that targeted the *TRPC3* exons are listed in Table 1. SgRNA sense and antisense oligos (20 nt for each) were phosphorylated and annealed, then ligated into a lentiCRISPRv2 vector (Addgene, 52961) cut with *Bsm*B I. The lentivirus production was performed in 293FT cells, as previously described (Sanjana et al., 2014). For infection, mESCs were plated at a density of 2.5×10^5 cells/well in a 6-well plate overnight at 37°C, after which 100 μL concentrated Scr or *TRPC3* sgRNA lentivirus (in PEG-it virus precipitation solution; LV810A-1, System Biosciences), was added to the cells in fresh medium containing 8 μg mL^{-1} polybrene. After 2 days, the infected mESCs were selected by incubation in fresh medium containing 3 μg mL^{-1} puromycin for 3–5 days. The puromycin-resistant mESCs were dissociated to form a single cell suspension, the cells were then serially diluted and transferred to a 96-well plate for the isolation of clonal cell lines. The extraction of genomic DNA, and the use of HRMA to detect indel mutations for these clonal cell lines, were performed as previously described (Bassett et al., 2013). The positive clonal cell lines in this first round of detections were selected for sequencing and for a second round of identification via Western blot. The PCR products spanning the sgRNA1 and sgRNA2 target sites were amplified from WT, Scr and single ESC clones with *TRPC3* sequencing primer 1 and 2, respectively (Table 1), and then subcloned into the pGEM-T easy vector (Promega, USA). Single bacteria colonies were selected for sequencing and the result was aligned with the WT *TRPC3* genomic sequence. The primers used for the HRMA and sequencing are listed in Table 1.

Western blot analysis

Western blot analysis was performed as described previously (Hao et al., 2014). The primary antibodies used to probe the polyvinylidene fluoride (PVDF) membrane (Millipore, USA) were TRPC3 (Alomone Labs, ACC-016, USA) and actin (Sigma-Aldrich Co. Ltd, A2066, USA), and they were used at dilutions of 1:500 and 1:5,000, respectively.

Immunocytochemistry

Cell fixation and immunolabeling were performed as described previously (Hao et al., 2014). The following mouse or rabbit primary antibodies were used: anti-TRPC3 (Alomone Labs, ACC-016); anti-Oct-3/4 (Santa Cruz Biotechnology, sc-5279, USA); anti-SSEA-1 (Santa Cruz Biotechnology, sc-21702); anti-Sox1 (R&D Systems, MAB-3369, USA); anti-Nestin (Santa Cruz Biotechnology, sc33677); anti-Tuj1 (R&D Systems, MAB-1195); anti-GFAP, (1:250; Sigma-Aldrich, G9269). The anti-Tuj1 antibody was used at a dilution of 1:1,000, whereas the others were used at 1:250. The appropriate Alexa Fluor-488/546 goat anti-mouse or rabbit IgG (Thermo Fisher Scientific) was then used at a dilution of 1:500. Images were acquired with a Leica TCS SP5 II laser scanning confocal system (Leica Microsystems, Germany) and analysed with Image J (NIH, http://imagej.nih.gov/ij/).

RNA isolation and quantitative RT-PCR (qRT-PCR)

The total RNA of mESCs and mESC-derived neural cells was extracted at the indicated time points with TRIzol Reagent (Thermo Fisher Scientific). Reverse transcription was performed with a High-capacity cDNA Reverse Transcription kit (Thermo Fisher Scientific), and qRT-PCR was performed with the primers listed in Table 1 using the SYBR Green I Master mix and a LightCycler 480 system (both from Roche, Switzerland). The relative level of gene expression was normalized to the expression of *GAPDH* with the LightCycler 480 software.

MTT assay

Cells were plated in a 96-well plate at a density of 1,000 cells/well and cultured for 4 days. On each day of culture within 4 days, MTT solution (20 μL of 5 mg mL^{-1}) was added to the cells in culture at 37°C for 4 h. These cells were then solubilized with DMSO and the amount of light generated was quantified in a light reader (Abs=570 nm).

PI analysis

Cell fixation and PI staining were performed as described

Table 1 Sequences of the primers used[a)]

Gene name	Direction	Primer sequences (5′→3′)
TRPC3 sgRNA1	Forward	CACCGGCGTGACAAGGGCCGGCGCC
	Reverse	AAACGGCGCCGGCCCTTGTCACGCC
TRPC3 sgRNA2	Forward	CACCGCAATCCAATAGCCGATGGCG
	Reverse	AAACCGCCATCGGCTATTGGATTGC
Scrambled sgRNA (Origene)	Forward	CACCGGCACTACCAGAGCTAACTCA
	Reverse	AAACTGAGTTAGCTCTGGTAGTGCC
TRPC3 HRMA1	Forward	ACTGATCAGGTCGTCGGA
	Reverse	ACGAGCACCGAACATGAA
TRPC3 HRMA2	Forward	CTGGTCGTGTTGGTCGTG
	Reverse	AACCACGGAGGGAAGGT
TRPC3 Sequencing 1	Forward	TGGAATCTGCATTTGGAAGGG
	Reverse	TTCTGGCCCATGTAGTCCAC
TRPC3 Sequencing 2	Forward	CTCCCAACAGTTTGTGGCTC
	Reverse	CTTCGTGTCTATCGTGGGGA
TRPC3	Forward	AGGCGCAGCAGTATGTGGA
	Reverse	GCCCAAAGCTCTCGTTTGC
TRPC1	Forward	AAGCTTTTCTTGCTGGCGT
	Reverse	CCCAAGCACATCTACGCAAT
TRPC2	Forward	TGGAAGCTCTTTGTTGCCTT
	Reverse	ACCAGAGACTCTCCCAGCAA
TRPC4	Forward	GCTGGAGGAGAAGACACTGG
	Reverse	GACCTGTCGATGTGCTGAGA
TRPC5	Forward	GTTCACAGCCAACTCCCATT
	Reverse	GGATCCCCTTGCAGTTGTTA
TRPC6	Forward	CAGGCCCAGATTGATAAGGA
	Reverse	CCAGCTTTGGCTCTAACGAC
TRPC7	Forward	CCTACGCCAGGGATAAGTG
	Reverse	AAGGCCACAAATACCATGA
GAPDH	Forward	CGTCCCGTAGACAAAATGGT
	Reverse	TTGATGGCAACAATCTCCAC
Nestin	Forward	AGATCGCTCAGATCCTGGAA
	Reverse	GAGTTCTCAGCCTCCAGCAG
Sox1	Forward	AGGAACACCCGGATTACAAGT
	Reverse	CGCTCATGTAGCCCTGAGAG
Oct4	Forward	AAGCCCTCCCTACAGCAGAT
	Reverse	CTGGGAAAGGTGTCCCTGTA
Tuj1	Forward	AGTCAGCATGAGGGAGATCG
	Reverse	GCTGATGACCTCCCAGAACT
NeuN	Forward	CAACTTATGGAGCGGTCGTG
	Reverse	TGGTTCCGATGCTGTAGGTT
TH	Forward	CTTCCGTGTGTTTCAGTGCA
	Reverse	AATGTCCTGGGAGAACTGGG
GFAP	Forward	GAGGGACAACTTTGCACAGG
	Reverse	TCCTCCAGCGATTCAACCTT
GAP65	Forward	TGGGTTTGAGGCACACATTG
	Reverse	TGCGCAAACTAGGAGGTACA
Olig1	Forward	CCAGACTTCTCTCCCAGACG
	Reverse	GCAACTACATCGCTCCTTGG

a) The sgRNA primers were used to generate the lentiCRISPR-*mTRPC3*, the HRMA primers were used to identify indels of the *mTRPC3* mutants, and the sequencing primers were used to amplify the *mTRPC3* sgRNA1/2 targeting sites and for sequencing.

previously (Hao et al., 2014). Cells were analyzed using a FACS Aria II system (BD Bioscience, USA) and data were analyzed with the FlowJo software (FlowJo LLC, USA).

Flow cytometry analysis of Sox1-GFP expression, apoptosis, and mitochondrial membrane potential

Sox1-GFP expression. Cells were fixed every other day from day 2 to day 14 with 4% PFA at room temperature for 20 min. They were then washed once and stored in PBS at 4°C before analysis.

Apoptosis. Cells were dissociated on day 0, 4, 6, or 10 of neural differentiation and washed once with PBS. The TUNEL assay was then performed with an *in situ* cell death detection kit (Roche). Cells were fixed with 4% PFA at room temperature for 1 h and washed once with PBS. After permeabilization, cells were stained with TdT reaction mixture at 37°C for 1 h in the dark. Cells were then washed with PBS twice before analysis.

Mitochondrial membrane potential. Cells were dissociated on day 0, 4, 6, or 10 of neural differentiation and washed once with PBS. They were then incubated with 250 nmol L^{-1} TMRM (Thermo Fisher Scientific) in HBSS buffer at 37°C for 30 min and washed twice before analysis.

AP staining

Pluripotent mESCs exhibit a high level of expression of AP. Thus, mESCs were cultured in ESGRO medium for 4 days, after which they were fixed for 2 min, and then incubated with the AP Detection Kit staining solution (Millipore) for 15 min at room temperature in the dark. The cells were washed with PBS and visualized with a Zeiss Axioskop upright microscope using a 20×/0.45 NA Plan Fluor dry objective lens.

Statistical analysis

Data were presented as mean±SE, and statistical analyses were conducted with the Student's *t*-test, such that $P<0.05$ was considered to be significant.

Compliance and ethics *The author(s) declare that they have no conflict of interest.*

Acknowledgements *We thank Prof. Austin Smith (Cambridge Stem Cell Institute, Cambridge, UK), for kindly providing us with the 46C cells. We also thank Ms. Mandy Chan (HKUST, Hong Kong) for her technical support and Prof. Jacques Haiech (University of Strasbourg, France) for his helpful comments about the project. This work was supported by the Hong Kong Research Grants Council (RGC) General Research Fund awards (662113, 16101714, 16100115), the ANR/RGC joint research scheme award (A-HKUST601/13), the Hong Kong Theme-based Research Scheme award (T13-706/11-1) and the Hong Kong Innovation and Technology Commission (ITCPD/17-9).*

Amaral, M.D., and Pozzo-Miller, L. (2007). TRPC3 channels are necessary for brain-derived neurotrophic factor to activate a nonselective cationic current and to induce dendritic spine formation. J Neurosci 27, 5179–5189.

Bassett, A.R., Tibbit, C., Ponting, C.P., and Liu, J.L. (2013). Highly efficient targeted mutagenesis of *Drosophila* with the CRISPR/Cas9 system. Cell Rep 4, 220–228.

Becker, E.B.E. (2014). The *Moonwalker* mouse: new insights into TRPC3 function, cerebellar development, and ataxia. Cerebellum 13, 628–636.

Becker, E.B.E., Oliver, P.L., Glitsch, M.D., Banks, G.T., Achilli, F., Hardy, A., Nolan, P.M., Fisher, E.M.C., and Davies, K.E. (2009). A point mutation in TRPC3 causes abnormal Purkinje cell development and cerebellar ataxia in moonwalker mice. Proc Natl Acad Sci USA 106, 6706–6711.

Beddington, R.S., and Robertson, E.J. (1989). An assessment of the developmental potential of embryonic stem cells in the midgestation mouse embryo. Development 105, 733–737.

Berridge, M.J., Bootman, M.D., and Roderick, H.L. (2003). Calcium: calcium signalling: dynamics, homeostasis and remodelling. Nat Rev Mol Cell Biol 4, 517–529.

Bradley, A., Evans, M., Kaufman, M.H., and Robertson, E. (1984). Formation of germ-line chimaeras from embryo-derived teratocarcinoma cell lines. Nature 309, 255–256.

Chuang, J.H., Tung, L.C., and Lin, Y. (2015). Neural differentiation from embryonic stem cells *in vitro*: an overview of the signaling pathways. World J Stem Cells 7, 437–447.

Dhara, S.K., and Stice, S.L. (2008). Neural differentiation of human embryonic stem cells. J Cell Biochem 105, 633–640.

Dulneva, A., Lee, S., Oliver, P.L., Di Gleria, K., Kessler, B.M., Davies, K.E., and Becker, E.B.E. (2015). The mutant *Moonwalker* TRPC3 channel links calcium signaling to lipid metabolism in the developing cerebellum. Hum Mol Genet 24, 4114–4125.

Eder, P., Poteser, M., Romanin, C., and Groschner, K. (2005). Na^+ entry and modulation of Na^+/Ca^{2+} exchange as a key mechanism of TRPC signaling. Pflugers Arch 451, 99–104.

Engel, M., Do-Ha, D., Muñoz, S.S., and Ooi, L. (2016). Common pitfalls of stem cell differentiation: a guide to improving protocols for neurodegenerative disease models and research. Cell Mol Life Sci 73, 3693–3709.

Esdar, C., Milasta, S., Maelicke, A., and Herget, T. (2001). Differentiation-associated apoptosis of neural stem cells is effected by Bcl-2 overexpression: impact on cell lineage determination. Eur J Cell Biol 80, 539–553.

Feng, S., Li, H., Tai, Y., Huang, J., Su, Y., Abramowitz, J., Zhu, M.X., Birnbaumer, L., and Wang, Y. (2013). Canonical transient receptor potential 3 channels regulate mitochondrial calcium uptake. Proc Natl Acad Sci USA 110, 11011–11016.

Fogel, B.L., Hanson, S.M., and Becker, E.B.E. (2015). Do mutations in the murine ataxia gene *TRPC3* cause cerebellar ataxia in humans? Mov Disord 30, 284–286.

Fusco, F.R., Martorana, A., Giampà, C., De March, Z., Vacca, F., Tozzi, A., Longone, P., Piccirilli, S., Paolucci, S., Sancesario, G., Mercuri, N.B., Bernardi, G. (2004). Cellular localization of TRPC3 channel in rat brain: preferential distribution to oligodendrocytes. Neurosci Lett 365, 137–142.

Hanson, S.M., Sansom, M.S.P., and Becker, E.B.E. (2015). Modeling suggests TRPC3 hydrogen bonding and not phosphorylation contributes to the ataxia phenotype of the *Moonwalker* mouse. Biochemistry 54, 4033–4041.

Hao, B., Lu, Y., Wang, Q., Guo, W., Cheung, K.H., and Yue, J. (2014). Role of STIM1 in survival and neural differentiation of mouse embryonic stem cells independent of Orai1-mediated Ca^{2+} entry. Stem Cell Res 12, 452–466.

Hao, B., Webb, S.E., Miller, A.L., and Yue, J. (2016). The role of Ca^{2+}

signaling on the self-renewal and neural differentiation of embryonic stem cells (ESCs). Cell Calcium 59, 67–74.
Hartmann, J., Dragicevic, E., Adelsberger, H., Henning, H.A., Sumser, M., Abramowitz, J., Blum, R., Dietrich, A., Freichel, M., Flockerzi, V., Birnbaumer, L., Konnerth, A. (2008). TRPC3 channels are required for synaptic transmission and motor coordination. Neuron 59, 392–398.
Hayashi, K., de Sousa Lopes, S.M.C., Tang, F., Lao, K., and Surani, M.A. (2008). Dynamic equilibrium and heterogeneity of mouse pluripotent stem cells with distinct functional and epigenetic states. Cell Stem Cell 3, 391–401.
Hipp, J., and Atala, A. (2008). Sources of stem cells for regenerative medicine. Stem Cell Rev 4, 3–11.
Jia, Y., Zhou, J., Tai, Y., and Wang, Y. (2007). TRPC channels promote cerebellar granule neuron survival. Nat Neurosci 10, 559–567.
Kwan, H.Y., Huang, Y., and Yao, X. (2006). Protein kinase C can inhibit TRPC3 channels indirectly via stimulating protein kinase G. J Cell Physiol 207, 315–321.
Leclerc, C., Néant, I., and Moreau, M. (2012). The calcium: an early signal that initiates the formation of the nervous system during embryogenesis. Front Mol Neurosci 5, 64.
Li, Y., Jia, Y.C., Cui, K., Li, N., Zheng, Z.Y., Wang, Y.Z., and Yuan, X.B. (2005). Essential role of TRPC channels in the guidance of nerve growth cones by brain-derived neurotrophic factor. Nature 434, 894–898.
Liang, J., Wang, Y.J., Tang, Y., Cao, N., Wang, J., and Yang, H.T. (2010). Type 3 inositol 1,4,5-trisphosphate receptor negatively regulates apoptosis during mouse embryonic stem cell differentiation. Cell Death Differ 17, 1141–1154.
Lichtenegger, M., and Groschner, K. (2014). TRPC3: a multifunctional signaling molecule. In: Mammalian Transient Receptor Potential (TRP) Cation Channels, B. Nilius, and V. Flockerzi, eds. (Berlin Heidelberg: Springer), pp. 67–84.
Lin, H.H., Bell, E., Uwanogho, D., Perfect, L.W., Noristani, H., Bates, T.J. D., Snetkov, V., Price, J., and Sun, Y.M. (2010). Neuronatin promotes neural lineage in ESCs via Ca^{2+} signaling. Stem Cells 28, 1950–1960.
Liu, S.P., Fu, R.H., Huang, S.J., Huang, Y.C., Chen, S.Y., Chang, C.H., Liu, C.H., Tsai, C.H., Shyu, W.C., Lin, S.Z. (2013). Stem cell applications in regenerative medicine for neurological disorders. Cell Transplant 22, 631–637.
Louhivuori, L.M., Jansson, L., Turunen, P.M., Jäntti, M.H., Nordström, T., Louhivuori, V., and Åkerman, K.E. (2015). Transient receptor potential channels and their role in modulating radial glial-neuronal interaction: a signaling pathway involving mGluR5. Stem Cells Dev 24, 701–713.
McNeish, J. (2004). Embryonic stem cells in drug discovery. Nat Rev Drug Discov 3, 70–80.
Minke, B., and Parnas, M. (2006). Insights on TRP channels from *in vivo* studies in *Drosophila*. Annu Rev Physiol 68, 649–684.
Nagasaka, R., Matsumoto, M., Okada, M., Sasaki, H., Kanie, K., Kii, H., Uozumi, T., Kiyota, Y., Honda, H., and Kato, R. (2017). Visualization of morphological categories of colonies for monitoring of effect on induced pluripotent stem cell culture status. Reg Ther 6, 41–51.
Nichols, J., Zevnik, B., Anastassiadis, K., Niwa, H., Klewe-Nebenius, D., Chambers, I., Schöler, H., and Smith, A. (1998). Formation of pluripotent stem cells in the mammalian embryo depends on the POU transcription factor Oct4. Cell 95, 379–391.
Orrenius, S., Gogvadze, V., and Zhivotovsky, B. (2015). Calcium and mitochondria in the regulation of cell death. Biochem Biophys Res Commun 460, 72–81.
Perry, S.W., Norman, J.P., Barbieri, J., Brown, E.B., and Gelbard, H.A. (2011). Mitochondrial membrane potential probes and the proton gradient: a practical usage guide. Biotech 50, 98–115.
Pinton, P., Giorgi, C., Siviero, R., Zecchini, E., and Rizzuto, R. (2008). Calcium and apoptosis: ER-mitochondria Ca^{2+} transfer in the control of apoptosis. Oncogene 27, 6407–6418.
Ran, F.A., Hsu, P.D., Wright, J., Agarwala, V., Scott, D.A., and Zhang, F. (2013). Genome engineering using the CRISPR-Cas9 system. Nat Protoc 8, 2281–2308.
Riccardi, C., and Nicoletti, I. (2006). Analysis of apoptosis by propidium iodide staining and flow cytometry. Nat Protoc 1, 1458–1461.
Sanjana, N.E., Shalem, O., and Zhang, F. (2014). Improved vectors and genome-wide libraries for CRISPR screening. Nat Meth 11, 783–784.
Soboloff, J., Spassova, M., Hewavitharana, T., He, L.P., Luncsford, P., Xu, W., Venkatachalam, K., van Rossum, D., Patterson, R.L., and Gill, D.L. (2007). TRPC channels: integrators of multiple cellular signals. Handb Exp Pharmacol (179), 575–591.
Štefková, K., Procházková, J., and Pacherník, J. (2015). Alkaline phosphatase in stem cells. Stem Cells Int 2015, 1–11.
Svobodova, B., and Groschner, K. (2016). Mechanisms of lipid regulation and lipid gating in TRPC channels. Cell Calcium 59, 271–279.
Tonelli, F.M.P., Santos, A.K., Gomes, D.A., da Silva, S.L., Gomes, K.N., Ladeira, L.O., and Resende, R.R. (2012). Stem cells and calcium signaling. Adv Exp Med Biol 740, 891–916.
Trebak, M., Vazquez, G., Bird, G.S.J., and Putney Jr., J.W. (2003). The TRPC3/6/7 subfamily of cation channels. Cell Calcium 33, 451–461.
Vazquez, G., Wedel, B.J., Trebak, M., St. John Bird, G., and Putney Jr., J. W. (2003). Expression level of the canonical transient receptor potential 3 (TRPC3) channel determines its mechanism of activation. J Biol Chem 278, 21649–21654.
Wei, W., Lu, Y., Hao, B., Zhang, K., Wang, Q., Miller, A.L., Zhang, L.R., Zhang, L.H., and Yue, J. (2015). CD38 is required for neural differentiation of mouse embryonic stem cells by modulating reactive oxygen species. Stem Cells 33, 2664–2673.
Weick, J.P., Johnson, M.A., and Zhang, S. (2009). Developmental regulation of human embryonic stem cell-derived neurons by calcium entry via transient receptor potential (TRP) channels. Stem Cells 27, 2906–2916.
Xu, X., Duan, S., Yi, F., Ocampo, A., Liu, G.H., and Izpisua Belmonte, J.C. (2013). Mitochondrial regulation in pluripotent stem cells. Cell Metab 18, 325–332.
Yeo, W., and Gautier, J. (2004). Early neural cell death: dying to become neurons. Dev Biol 274, 233–244.
Ying, Q.L., and Smith, A.G. (2003). Defined conditions for neural commitment and differentiation. Meth Enzymol 365, 327–341.
Ying, Q.L., Stavridis, M., Griffiths, D., Li, M., and Smith, A. (2003). Conversion of embryonic stem cells into neuroectodermal precursors in adherent monoculture. Nat Biotechnol 21, 183–186.
Yu, H.M., Wen, J., Wang, R., Shen, W.H., Duan, S., and Yang, H.T. (2008). Critical role of type 2 ryanodine receptor in mediating activity-dependent neurogenesis from embryonic stem cells. Cell Calcium 43, 417–431.
Zhang, Z.H., Lu, Y.Y., and Yue, J. (2013). Two pore channel 2 differentially modulates neural differentiation of mouse embryonic stem cells. PLoS ONE 8, e66077.